

# НАУКИ О ЗЕМЛЕ

УДК 553.491.8:553.062

DOI 10.21440/2307-2091-2017-2-7-12

## CHEMICAL AND Os-ISOTOPE COMPOSITION OF PLATINUM-GROUP MINERAL ASSEMBLAGES FROM THE KIMBERLEY CONGLOMERATE FORMATION (WITWATERSRAND BASIN, SOUTH AFRICA)

I. Yu. Badanina, K. N. Malitch, A. V. Antonov, I. N. Kapitonov, V. V. Khiller, S. M. Tuganova, R. K. W. Merkle

### Химический и Os-изотопный состав минеральных ассоциаций платиноидов конгломератной формации Кимберли (Витватерсрандский бассейн, Южная Африка)

И. Ю. Баданина, К. Н. Малич, А. В. Антонов, И. Н. Капитонов, В. В. Хиллер, С. М. Туганова, Р. К. В. Меркль

Комплексные Os–Au–U палеороссыпи Витватерсрандского бассейна, известные как Витватерсрандские рифы, разрабатываются уже более ста лет. С целью уточнения источников рудного вещества, продолжительности и условий образования платиноидной минерализации Витватерсрандского бассейна в статье обсуждаются оригинальные данные по химическому и Os-изотопному составу в минералах платиновой группы (МПГ) из золотоносной конгломератной формации Кимберли, расположенной в верхнем отделе Центрального Ранда (Turffontein Subgroup of the Central Rand Group). Для исследования платиноидной минерализации применен комплекс методов, включающий рентгеноспектральный микронализ, лазерную абляцию и масс-спектрометрию с ионизацией в индуктивно-связанной плазме. Величина  $^{187}\text{Os}/^{188}\text{Os}$  в единичных зернах МПГ различного состава (рутения, осмия, иридия, рутениридосмина, лаурита, эрликманита, поликомпонентных твердых растворов системы Ru–Os–Ir–Pt ( $\pm$  Fe)) варьирует в пределах от  $0,10481 \pm 0,00006$  до  $0,10895 \pm 0,00006$ ;  $^{187}\text{Re}/^{188}\text{Os}$  менее 0,0004. Изученная выборка МПГ образована двумя основными группами, которые характеризуются средними значениями  $^{187}\text{Os}/^{188}\text{Os}$ , равными  $0,10510 \pm 0,00026$  ( $n = 11$ ) и  $0,10682 \pm 0,00046$  ( $n = 23$ ) с подчиненным кластером значений  $^{187}\text{Os}/^{188}\text{Os} = 0,10871 \pm 0,00034$  ( $n = 2$ ). Для существующих Os-содержащих МПГ в составе полиминеральных агрегатов выявлен одинаковый Os-изотопный состав для Ir-содержащего осмия и эрликманита ( $^{187}\text{Os}/^{188}\text{Os} = 0,10482 \pm 0,00002$  и  $0,10483 \pm 0,00002$  соответственно), Os–Ru–Ir–Pt сплава и лаурита ( $^{187}\text{Os}/^{188}\text{Os} = 0,10528 \pm 0,00002$  и  $0,10533 \pm 0,00003$  соответственно).  $^{187}\text{Os}/^{188}\text{Os}$  возрасты МПГ, рассчитанные с использованием модели хондритового резервуара CHUR (Chen et al., 1998), варьируют в пределах 2,73–3,33 млрд лет. Средние модельные возраста  $T_{\text{MA}}^{\text{CHUR}}$  для двух основных групп МПГ оказались равными 3,250  $\pm$  0,035 и 3,018  $\pm$  0,062 млрд лет. Третий возрастной кластер  $2,762 \pm 0,046$  млрд лет образован подчиненной по распространенности группой МПГ. Новые результаты свидетельствуют в пользу: 1) высокотемпературной природы образования Ru–Os–Ir–Pt сплавов, поликомпонентных твердых растворов системы Ru–Os–Ir–Pt ( $\pm$  Fe) и RuOs сульфидов, 2) сходства начального изотопного состава осмия в существующих Os-содержащих сплавах и Ru–Os сульфидах, 3) субхондритового архейского источника рудного вещества и 4) обломочного происхождения изученных МПГ.

**Ключевые слова:** Os–Ru–Ir–Pt сплавы; Ru–Os сульфиды; Os-изотопный состав; условия образования; конгломератная формация Кимберли; Витватерсрандский бассейн; Южная Африка.

Complex Os–Au–U paleoplacers of the Witwatersrand basin, known as the Witwatersrand reefs, have been mined for more than a hundred years. In order to clarify the sources of ore matter, the duration and conditions for formation of platinum-group element (PGE) mineralization this study presents the original data on chemical and Os-isotopic composition in platinum-group minerals (PGM) derived from the Kimberley gold-bearing conglomerate formation located in the upper section of the Central Rand (Turffontein Subgroup of The Central Rand Group). The study employed a number of analytical techniques including electron microprobe analysis, laser ablation and mass spectrometry with ionization in inductively coupled plasma. The  $^{187}\text{Os}/^{188}\text{Os}$  value in individual PGM grains of various compositions (rutheum, osmium, iridium, rutheniridossime, laurite, erlichmanite, unnamed polycomponent solid solutions of the Ru–Os–Ir–Pt ( $\pm$  Fe) system) was found to range from  $0,10481 \pm 0,00006$  to  $0,10895 \pm 0,00006$ , and  $^{187}\text{Re}/^{188}\text{Os}$  lower than 0,0004. The studied PGM assemblage is represented by two main groups with mean  $^{187}\text{Os}/^{188}\text{Os}$  values of  $0,10510 \pm 0,00026$  ( $n = 11$ ) and  $0,10682 \pm 0,00046$  ( $n = 23$ ), and a subordinate  $^{187}\text{Os}/^{188}\text{Os}$  cluster of  $0,10871 \pm 0,00034$  ( $n = 2$ ). The Os-isotope results identify similar  $^{187}\text{Os}/^{188}\text{Os}$  values for coexisting Os-bearing PGM pairs including Os-rich alloy and erlichmanite (i. e.,  $0,10482 \pm 0,00002$  and  $0,10483 \pm 0,00002$ , respectively), Os–Ru–Ir–Pt alloy and laurite ( $0,10528 \pm 0,00002$  and  $0,10533 \pm 0,00003$ , respectively).  $^{187}\text{Os}/^{188}\text{Os}$  ages of the PGM, calculated relative to a chondrite universal reservoir (CHUR) model (Chen et al., 1998), vary between 2,73 and 3,33 Ga. Two main PGM groups have mean model  $T_{\text{MA}}^{\text{CHUR}}$  ages of  $3,250 \pm 0,035$  and  $3,018 \pm 0,062$  Ga. Subordinate-PGM group is characterized by the third age cluster ( $2,762 \pm 0,046$  Ga). The obtained results are consistent with: (i) high-temperature formation of the studied Ru–Os–Ir–Pt alloys, polycomponent solid solutions of the Ru–Os–Ir–Pt ( $\pm$  Fe) system and Ru–Os sulfides, (ii) similarity of the initial Os-isotope composition in coexisting Os-rich alloys and Ru–Os sulfides, (iii) subhondritic Archean source of platinum-group elements (PGE), and (iv) clastic origin of the studied PGM.

**Keywords:** Os–Ru–Ir–Pt alloys; Ru–Os sulfides; Os-isotopic composition; formation conditions; Kimberley conglomerate formation; Witwatersrand basin; South Africa.

### Introduction

The complex Os–Au–U paleoplacers of the Witwatersrand Basin, known as the Witwatersrand reefs [1], have been mined for more than 100 years. They are one of the main suppliers of gold and osmium to the world market. Osmium-rich platinum-group minerals (PGMs) are obtained as a co-product during gold mining within the goldfields of the Witwatersrand Basin. PGMs described *in situ* in the Witwatersrand lithified formations or in production concentrates have typical sizes ranging from  $\sim 70\mu\text{m}$  to  $\sim 150\mu\text{m}$ . The characteristics of their material composition and the conditions for the formation of PGM assemblages are given in a number of publications [2–4 etc.]. First Os-isotopic data on Ru–Os–Ir alloys from the Witwatersrand basin revealed significant variations of  $^{187}\text{Os}/^{188}\text{Os}$  values (0,0987 to 0,1649 [3, 5, 6]).

In order to clarify the source of the ore material, the duration and conditions of formation of Os-bearing PGMs at Witwatersrand we discuss the original data on the chemical and isotopic composition of Os-bearing alloys and sulfides from the Kimberley conglomerate formation (Fig. 1). The information on genetic features of the formation of PGM data is given taking into account the revealed composition of rarely occurring unnamed polycomponent solid solutions of the Ru–Os–Ir–Pt ( $\pm$  Fe) system. The new results are consistent with: (i) high-temperature formation of Ru–Os–Ir–Pt alloys, unnamed polycomponent solid solutions of the Ru–Os–Ir–Pt ( $\pm$  Fe) system and Ru–

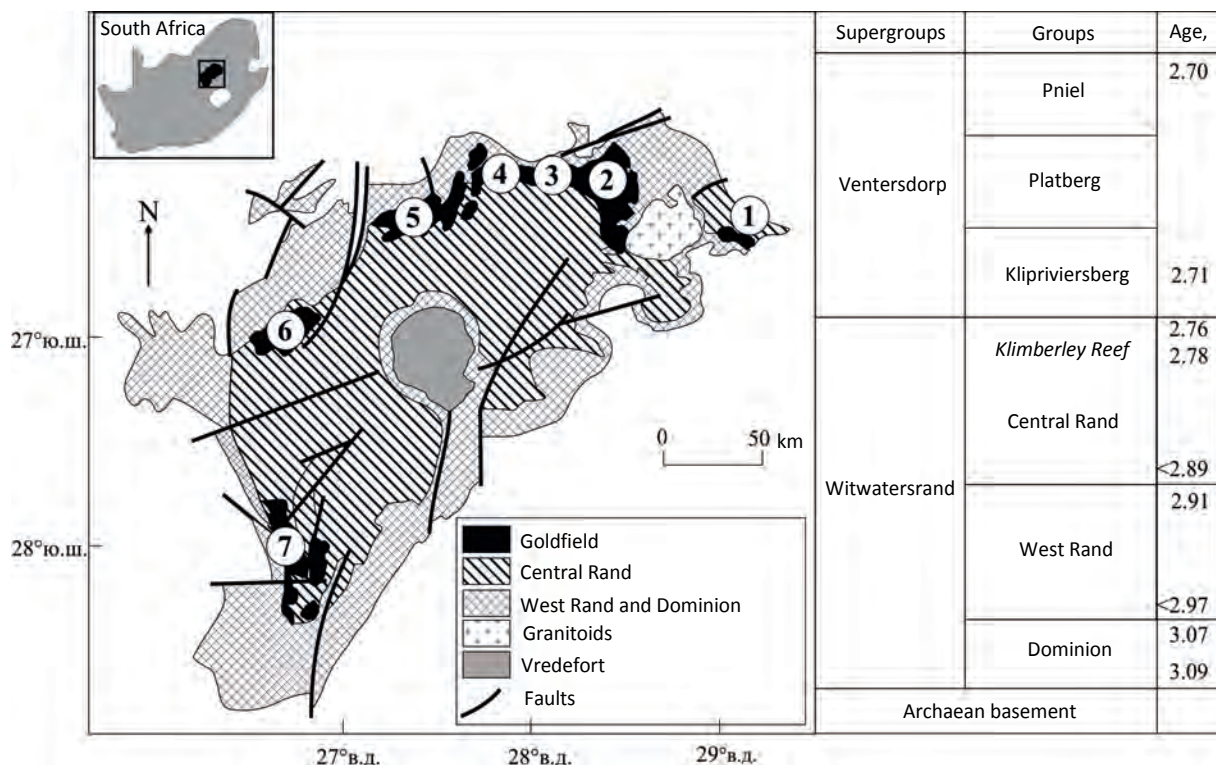


**Figure 1.** Schematic map of the Witwatersrand basin and location of the main goldfields (1 – Evander, 2 – East Rand, 3 – Central Rand, 4 – West Rand, 5 – Carletonville, 6 – Klerksdorp, 7 – Welkom) after [7]. The stratigraphic column shows the position of the Kimberley gold-bearing conglomerate formation (Kimberley Reef), from which the PGMs were taken for our study.

Os sulfides, (ii) the subhondritic Archaeon source of platinum-group elements (PGE), and (iii) the clastic origin of the studied PGMs.

#### Subject of research and geological characteristics

The Witwatersrand Basin is an erosional remnant of a much larger basin, formed over a long period of time (3074–2714 Ma ago) in the central and southern parts of the Kaapvaal Craton [8, 9]. It extends in the northeast – southwest direction for 300 km, with a width of about 100 km, and consists of a thick (> 7 km) succession of quartzites, slates, and conglomerates that have a distinctive rhythmic structure [1]. In the section of sedimentary strata, the conglomerates make up less than 0.2% of the total thickness, forming 16 separate horizons (reefs) bearing gold and uranium mineralization accompanied by PGMs. The main resources of gold and PGE are restricted to conglomerates of the Central Rand Group; their mining is carried out by a mine method within seven goldfields: Evander, East Rand, Central Rand, West Rand, Carletonville, Klerksdorp and Welkom (Fig. 1).

A representative selection of 450 PGM grains in the range from 60 to 150 micrometers is derived from a production concentrate from the Kimberley gold-bearing conglomerate formation (or the Kimberley Reef) located in the upper part of the Central Rand Group (Turffontein Subgroup of The Central Rand Group) [10]. The time interval of deposition of the Central Rand sediments did not exceed 230 Ma and is constrained by the overlying volcanic rocks of the Ventersdorp Supergroup dated at ~ 2710 Ma [8, 11].

#### Analytical methods

Chemical composition of PGMs was studied using electron microprobe analysis (ARL-SEMQ, University of Leoben, Austria; Cam-Scan MX2500, VSEGEI, St. Petersburg; CAMECA SX 100, IGG UB RAS, Ekaterinburg). For quantitative analyses, an accelerating voltage of 15 kV, a beam current of 20 nA, and a beam diameter of approximately 1–2 µm was used. The following X-ray spectral lines and standards were employed: OsMa, IrLa, RuLa, RhLa, PtLa, PdLβ, NiKa (all native element standards), FeKa, CuKa, SKa (all chalcopyrite), AsLa (InAs alloy). Corrections were performed for the interferenc-

es involving Ru–As, Ru–Rh and Ir–Cu (RuLa for AsLa, RuLβ for Rh La, IrL1 for CuKa). In total, 550 analyses were performed. The initial Os-isotope compositions in individual PGMs were determined using laser ablation attached to a multicollector inductively coupled plasma mass spectrometry (MC ICP-MS, mass spectrometer Neptune at the All-Russian Geological Research Institute, St. Petersburg). Ablation was carried out with a spot size ranging from 30 to 80 µm, a pulse frequency of 8–20 Hz, and typical run duration of 40–72 s. Measured isotope ratios were normalized by taking into account mass-fractionation effects. The mass-bias correction was performed using  $^{189}\text{Os}/^{188}\text{Os} = 1.21978$  [12]. In total, 36 analyses were carried out. A detailed description of analytical methods is given in a number of papers [13–17].

#### Results of the study

*Chemical composition of Os-containing alloys and Ru–Os sulfides.* Ru–Os–Ir ( $\pm$  Pt) alloys in monomineralic grains or polymineralic assemblages (Fig. 2) form the main population of the PGMs studied. For Ru–Os–Ir ( $\pm$  Pt) alloys, significant intra-grain compositional variations have been observed. According to the nomenclature of D. Harris and L. Cabri [18], minerals of ruthenium predominate over the minerals of osmium, iridium and rutheniridosmine (Fig. 3, Table 1, an. 1, 12). Ru–Os sulfides found in polymineralic grains (Fig. 2, f) correspond to laurite and erlichmanite, which form a continuous series of solid solutions (Ru# varies from 100 to 24, Table 1, an. 13, 14). The uncommon polycomponent solid solutions of the Ru–Os–Ir–Pt ( $\pm$ Fe) system have been determined to be present both as monomineralic and polymineralic grains (Fig. 2, a–e). Polyphase aggregates commonly contain a core formed by unnamed polycomponent solid solutions of the Ru–Os–Ir–Pt ( $\pm$  Fe) system enveloped by sperrylite ( $\text{PtAs}_2$ ), and rarely by Ru–Os sulfides or Ru–Os–Ir–Rh sulfoarsenides. Among the polycomponent solid solutions of the Ru–Os–Ir–Pt ( $\pm$ Fe) system the following varieties have been identified in the order of their prevalence: (Ru, Os, Ir, Pt), (Ru, Pt, Os, Ir), (Ru, Os, Pt, Ir), (Ru, Ir, Os, Pt, Fe), (Ru, Pt, Ir), (Ru, Pt, Fe), (Os, Ru, Ir, Pt), (Os, Ru, Ir, Pt), (Ir, Os, Ru, Pt), (Ru, Pt), (Pt, Ru, Fe), (Pt, Ru, Os, Fe), (Pt, Fe, Ru), (Pt, Ru) and others (Fig. 2, a–e, Table 1, an. 2–11).

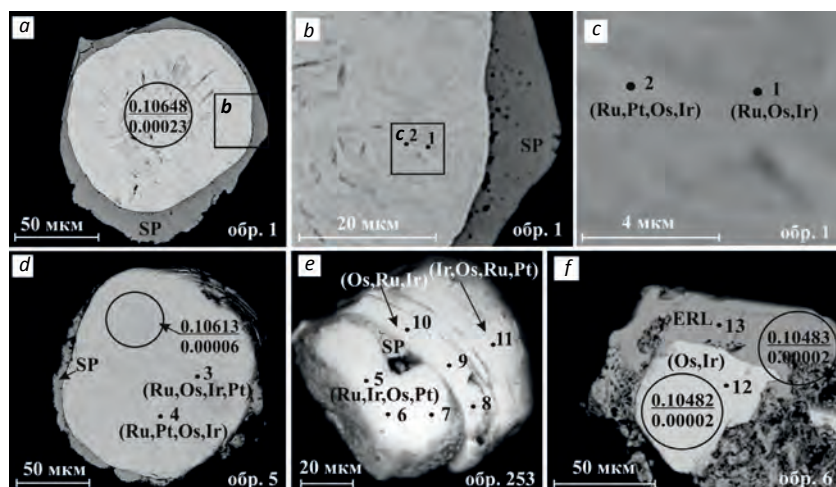


**Figure 2.** Back-scattered electron images showing the internal textures of the PGM assemblages from the Kimberley conglomerate formation. Numbers 1–13 denote areas of electron microprobe analyses corresponding to the same numbers in Table 1. Circles indicate the location of Os-isotope analyses; numbers in the numerator and denominator correspond to the  $^{187}\text{Os}/^{188}\text{Os}$  value and the measurement error, respectively.

The initial Os isotopic composition of Os-bearing alloys and Ru–Os sulfides. The  $^{187}\text{Os}/^{188}\text{Os}$  value in individual PGM grains of different compositions (ruthenium, osmium, iridium, laurite, erlichmanite and other minerals of the Ru–Os–Ir–Pt–Fe system) varies from  $0.10481 \pm 0.00006$  to  $0.10895 \pm 0.00006$  (Table 2), and  $^{187}\text{Re}/^{188}\text{Os}$  less than 0.0004. According to the calculations carried out with ISOPLOT program [19], two main groups of PGMs can be identified (Table 3, Fig. 4, a), with the mean  $^{187}\text{Os}/^{188}\text{Os}$  values of  $0.10510 \pm 0.00026$  ( $n = 11$ ) and  $0.10682 \pm 0.00046$  ( $n = 23$ ), respectively (calculated errors are within 95% confidence level). The third subordinate cluster is characterized by a mean  $^{187}\text{Os}/^{188}\text{Os}$  of  $0.10871 \pm 0.00034$  ( $n = 2$ ). No correlation between chemical composition and isotope content of the samples was discovered within the limits of the experimental precision. Osmium-isotope compositions of optically homogeneous PGM crystals range, as a rule, over the same interval as those of PGM associations consisting of a core and a rim (Table 2). The Os-isotope results identify similar  $^{187}\text{Os}/^{188}\text{Os}$  values for coexisting Os-bearing PGM pairs including Os-rich alloy and erlichmanite (i.e.,  $0.10482 \pm 0.00002$  and  $0.10483 \pm 0.00002$ , respectively, Fig. 2, f; Table 2, an. 5, 6), Os–Ru–Ir–

Pt alloy and laurite ( $0.10528 \pm 0.00002$  and  $0.10533 \pm 0.00003$ , respectively, Table 2, an. 12, 13). Model ages of PGMs, calculated relative to a chondrite universal reservoir (CHUR) model [20], vary within 2.73–3.33 Ga (Table 2). Two main PGM groups have mean model  $T_{\text{MA}}^{\text{CHUR}}$  ages of  $3.250 \pm 0.035$  and  $3.018 \pm 0.062$  Ga, whereas subordinate PGM group is characterized by the third age cluster ( $2.762 \pm 0.046$  Ga, Table 3, Fig. 4, b).

#### Discussion of results

To explain the origin of more than 96,000 tons of gold contained in the basin [22], the three models / hypotheses have been proposed.

1. Placer model assumes that noble metal mineralization is a detrital material from an older granite-greenstone source area, which has been mechanically transported into the basin and concentrated by fluvial/deltaic processes [23–27 etc.].

2. The modified placer model assigns a significant role to hydrothermal processes for most of the gold/PGM. In this model, alluvial gold and associated PGMs should have been mobilized by hydrothermal or metamorphic fluids, and locally re-precipitated together with other minerals [9, 28, 29 etc.].

**Table 1. Chemical compositions of platinum-group minerals from the Kimberley conglomerate formation.**

Analysis	1	2	3	4	5	6	7	8	9	10	11	12	13	14
Sample	1	1	5	5	253	253	353	253	253	253	253	6	6	101
Figure 2	b, c	b, c	d	d	e	e	e	e	e	e	e	f	f	–
Wt. %														
Fe	0.00	1.39	0.25	0.54	2.72	2.43	2.56	0.48	0.34	0.24	2.99	0.16	0.00	0.00
Ni	0.00	0.00	0.00	0.58	0.23	0.00	0.17	0.30	0.00	0.18	0.19	0.00	0.00	0.00
Cu	0.00	0.00	0.00	0.00	0.00	0.00	0.00	0.00	0.00	0.00	0.00	0.00	0.00	0.00
Ru	40.46	32.97	35.76	28.38	16.98	17.10	16.56	17.76	18.05	16.78	13.87	0.00	8.23	57.90
Rh	0.00	0.00	2.00	2.19	0.17	0.14	0.25	0.16	0.14	0.14	0.14	0.00	0.00	2.19
Os	28.00	23.36	34.21	19.50	28.42	30.48	29.41	46.06	45.94	45.98	29.04	64.63	49.07	0.44
Ir	25.97	18.28	16.77	14.15	30.68	30.13	30.90	26.21	27.03	27.58	30.05	34.34	16.17	0.64
Pt	4.51	24.00	11.02	34.66	20.31	18.95	19.73	9.03	8.41	8.84	23.14	0.00	0.00	0.00
S	0.00	0.00	0.00	0.00	0.00	0.00	0.00	0.00	0.00	0.00	0.00	26.49	38.29	
Total	98.94	100.00	100.01	100.00	99.51	99.23	99.58	100.00	99.91	99.74	99.42	99.13	99.96	99.46
Atom %														
Fe	0.00	3.60	0.64	1.43	7.67	6.93	7.21	1.40	1.00	0.71	8.59	0.55	0.00	0.00
Ni	0.00	0.00	0.00	1.46	0.62	0.00	0.46	0.83	0.00	0.51	0.52	0.00	0.00	0.00
Cu	0.00	0.00	0.00	0.00	0.00	0.00	0.00	0.00	0.00	0.00	0.00	0.00	0.00	0.00
Ru	56.72	47.13	50.45	41.58	26.44	26.94	26.41	28.53	29.21	27.43	22.03	0.00	6.52	31.93
Rh	0.00	0.00	2.77	3.15	0.26	0.21	0.37	0.25	0.23	0.22	0.21	0.00	0.00	1.19
Os	20.86	17.75	25.64	15.18	23.51	25.51	24.33	39.33	39.51	39.94	24.51	65.18	20.64	0.13
Ir	19.14	13.74	12.44	10.90	25.12	24.95	25.30	22.14	23.00	23.70	25.10	34.27	6.73	0.18
Pt	3.28	17.78	8.05	26.30	16.38	15.46	15.92	7.52	7.05	7.49	19.04	0.00	0.00	0.00
S	0.00	0.00	0.00	0.00	0.00	0.00	0.00	0.00	0.00	0.00	0.00	66.11	66.57	
Ru#	–	–	–	–	–	–	–	–	–	–	–	–	24	100

Note. Concentrations of Pd, Cu, and As are below the detection limit of EMPA; Ru# of Ru–Os of sulfides is equal to  $100 * \text{Ru at. \%} / (\text{Ru} + \text{Os}) \text{ at. \%}$ .  
1 – (Ru, Os, Ir), 2 and 4 – (Ru, Pt, Os, Ir), 3 and 6 – (Ru, Os, Ir, Pt), 4 and 7 – (Ru, Ir, Os, Pt), 8–10 – (Os, Ru, Ir), 11 – (Ir, Os, Ru, Pt), an. 12 – Ir-bearing osmium, an. 13 – erlichmanite, an. 14 – laurite.

Table 2. Initial Os-isotope composition and model  $T_{MA}^{CHUR}$  age of PGMs from the Kimberley conglomerate formation.

№ analysis	Sample number, Figure number	Mineral assemblages	$^{187}\text{Os}/^{188}\text{Os}$	$1\sigma$	$T_{MA}^{CHUR}$ , Ga	$1\sigma$
1	W1-1, fig. 2, a–c	(Ru, Pt, Os, Ir) + (Ru, Os, Ir) + SP	0.10648	0.00029	3.064	0.039
2	W1-2	(Ru, Ir, Os, Pt) + SP	0.10651	0.00010	3.060	0.014
3	W1-3	(Os, Ru, Ir, Pt) + SP	0.10657	0.00008	3.051	0.011
4	W1-5, fig. 2, d	(Ru, Os, Pt, Ir) + (Ru, Pt, Os, Ir) + SP	0.10613	0.00006	3.111	0.008
5	W1-6_1, fig. 2, f	(Os, Ir) + ERL	0.10482	0.00002	3.287	0.002
6	W1-6_2, fig. 2, f	ERL + (Os, Ir)	0.10483	0.00002	3.286	0.002
7	W1-7	(Ru, Os, Ir, Pt) + SP	0.10565	0.00004	3.175	0.006
8	W1-9	(Ru, Os, Pt, Ir) + SP	0.10500	0.00006	3.263	0.008
9	W1-12	(Ru, Ir, Pt, Os) + SP	0.10595	0.00012	3.135	0.016
10	W1-15	(Ru, Ir, Pt, Os) + SP	0.10481	0.00006	3.288	0.008
11	W1-17	(Ru, Os, Ir, Pt) + SP	0.10749	0.00006	2.927	0.007
12	W1-20_1	(Os, Ru, Ir, Pt) + LR + SP	0.10528	0.00002	3.225	0.002
13	W1-20_2	LR + (Os, Ru, Ir, Pt) + SP	0.10533	0.00003	3.218	0.004
14	W1-24	(Ru, Pt, Os, Ir) + LR + SP	0.10512	0.00013	3.247	0.017
15	W1-25	(Ru, Pt, Ir, Os) + SP	0.10694	0.00020	3.002	0.027
16	W1-26	(Ru, Os, Ir, Pt) + (Ru, Ir, Pt, Os) + SP	0.10678	0.00011	3.023	0.015
17	W1-27	(Ru, Os, Ir, Pt) + SP	0.10732	0.00015	2.950	0.020
18	W1-28	(Ru, Pt, Os, Ir) + SP	0.10774	0.00031	2.893	0.042
19	W1-33	(Ru, Os, Ir) + (Ru, Os, Ir, Pt) + SP	0.10685	0.00010	3.014	0.014
20	W1-37	(Ru, Pt, Ir, Os) + SP	0.10619	0.00017	3.103	0.022
21	W1-51	(Os, Ru, Ir) + PTS-IRS	0.10736	0.00003	2.945	0.005
22	W1-52	(Ru, Pt, Os, Ir) + SP	0.10691	0.00005	3.006	0.006
23	W1-57	(Ru, Os, Ir, Pt) + SP	0.10504	0.00005	3.257	0.006
24	W1-58	(Ru, Os, Ir, Pt) + SP	0.10641	0.00006	3.073	0.008
25	W1-62	(Ru, Os, Pt, Ir) + SP	0.10713	0.00006	2.976	0.008
26	W1-63	(Ru, Pt, Os, Ir) + (Pt, Ru, Os, Fe) + SP	0.10521	0.00002	3.235	0.003
27	W1-68	LR	0.10496	0.00005	3.268	0.007
28	W1-69	(Ru, Pt, Ir, Os) + SP	0.10704	0.00063	2.988	0.085
29	W1-71	(Pt, Ru, Os, Fe)	0.10847	0.00013	2.795	0.017
30	W1-75	(Ru, Pt, Os, Ir)	0.10710	0.00006	2.980	0.008
31	W1-80	(Ru, Os, Ir, Pt) + LR	0.10691	0.00005	3.006	0.006
32	W1-82	(Ru, Pt, Ir, Os) + SP	0.10679	0.00006	3.022	0.008
33	W1-84	(Ru, Pt, Os, Ir) + SP	0.10895	0.00006	2.730	0.009
34	W1-85	(Ru, Pt, Ir) + SP	0.10713	0.00012	2.976	0.016
35	W1-89	(Os, Ru, Ir) + SP	0.10626	0.00005	3.093	0.006
36	W1-91	(Ru, Ir, Pt, Os) + SP	0.10684	0.00011	3.015	0.015

Note.  $T_{MA}^{CHUR}$  is the model age calculated taking into account the isotopic composition of osmium in CHUR after [20] and the decay constant of  $^{187}\text{Re}$ ,  $\lambda = 1.666 \times 10^{-11}$  year $^{-1}$  according to [21]. (Ru, Os, Ir) – ruthenium; (Ru, Os, Pt, Ir), (Ru, Pt, Os, Ir), (Ru, Os, Ir, Pt), (Ru, Ir, Os, Pt), (Ru, Ir, Pt, Os), (Ru, Pt, Ir), (Ru, Pt), (Pt, Ru, Os, Fe) – polycomponent solid solutions of the Ru–Os–Ir–Pt ( $\pm$  Fe) system; (Os, Ir), (Os, Ir, Ru) – osmium; LR – laurite; ERL – erlichmanite; SP – sperrylite; PTS-IRS – Pt–Ir sulfarsenides of the platarsite–irarsite series.

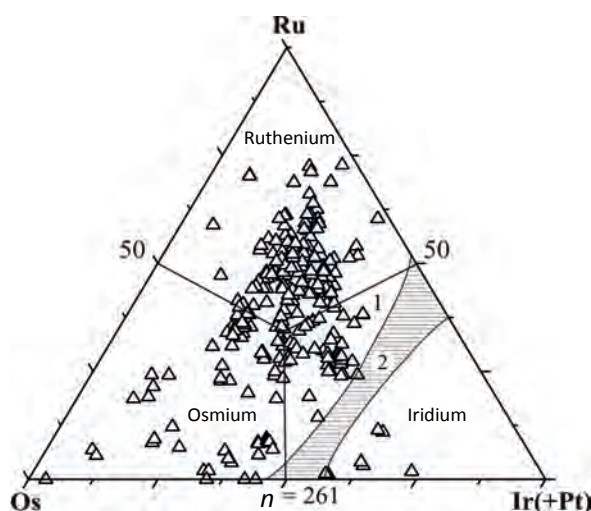


Figure 3. Chemical composition of PGMs from the Kimberley conglomerate formation in the diagram (at. %) Ru–Os–Ir(+Pt). 1 and 2 denote areas of rutheniridosmine and miscibility gap, respectively [18].

3. The metamorphic / hydrothermal model proposes that noble metal mineralization was transported in solutions from outside the basin by metamorphic or hydrothermal fluids after the formation of the basin [30–33 etc.].

The possibility of determining the time of formation of different ore minerals allowed testing these hypotheses [3, 6, 34–37]. During the studying of the Re–Os isotope system of gold and pyrite, several studies established [34, 35] that the isochronal age of ore minerals turned out to be older than the age of the basin deposits, consistent with their clastic origin. Pilot studies of Ru–Os–Ir alloys from the Evander goldfield came to similar conclusions [3, 5]. Studies aiming on pyrite dating [36, 37] established that this mineral is younger than the age of the basin deposits and interpreted the results in the framework of the modified placer model, which is consistent with some results of the study of Os–Ir Witwatersrand alloys [6].

In contrast to the previously obtained results on mineralogical characteristics of the PGE mineralization of Witwatersrand [2, 38 etc.], we documented a considerable occurrence of ruthenium-rich alloys, which predominate over osmium minerals [(Os, Ru, Ir), (Os, Ir) and Os], iridium [(Ir, Os), (Ir, Ru, Os) and Ir], rutheniridosmine (Ir, Os, Ru), Ru–Os sulfides and other PGMs. Ru–Os–Ir ( $\pm$  Pt) alloys of the Kimberley conglomerate formation are characterized by lower

**Table 3.** Os-isotopic statistics for the PGM groups of the Kimberley conglomerate formation.

PGM group	$^{187}\text{Os}/^{188}\text{Os}$					Model $T_{\text{MA}}^{\text{CHUR}}$ age		
	Mean	Standard deviation	Minimum	Maximum	Average	Standard deviation	Minimum	Maximum
1, $n = 11$	0.10510	0.00026	0.10481	0.10565	3.250	0.035	3.175	3.288
2, $n = 23$	0.10682	0.00046	0.10595	0.10774	3.018	0.062	2.893	3.135
3, $n = 2$	0.10871	0.00034	0.10847	0.10895	2.762	0.046	2.730	2.795

than typical bulk  $(\text{Os} + \text{Ir})/(\text{Ru} + \text{Pt} + \text{Rh})$  value, mainly due to the elevated contents of Ru and Pt in Ru–Os–Ir–Pt alloys.

According to J. Bird and W. Basset [39], the presence of a ruthenium trend for chemical compositions of the Ru–Os–Ir ( $\pm$  Pt) alloys of the Witwatersrand Basin (Fig. 3) indicates the formation of these minerals under high pressures within mantle-deep interiors. The high-temperature nature of the formation of Ru–Os sulfides has been confirmed experimentally [40]. The upper thermal stability of laurite was estimated at 1200–1250 °C and  $\log f(S_2) = -1$ ; whereas the upper thermal stability of laurite in equilibrium with Os-rich alloys was estimated at 1200–1250 °C and  $\log f(S_2)$  ranging from –0.39 to –0.07 [40].

Since the  $^{187}\text{Re}/^{188}\text{Os}$  value in all the studied samples was less than 0.0004, the isotopic effects caused by *in situ* radioactive decay of  $^{187}\text{Re}$  is negligible. Variations in the isotopic composition of osmium in individual PGM grains from the Kimberley gold-bearing conglomerate formation ( $^{187}\text{Os}/^{188}\text{Os}$  from 0.10481 to 0.10895) turned out to be close to Os-isotope compositions of the PGM of the Evander and Welkom goldfields located respectively in the eastern and southern parts of the Witwatersrand basin [3, 5, 6]. However, the PGMs of the Welkom goldfield are characterized by a wider range of  $^{187}\text{Os}/^{188}\text{Os}$ , including the suprachondritic  $^{187}\text{Os}/^{188}\text{Os}$  values (0.1056–0.1649 [3, 6]). Platinum-group minerals from the Evander goldfield mainly have subchondritic  $^{187}\text{Os}/^{188}\text{Os}$  values (0.1052–0.1091,  $n = 22$  [3, 5]), with a subset of least ‘radiogenic’ subchondritic  $^{187}\text{Os}/^{188}\text{Os}$  values found for the three PGM grains within the Witwatersrand basin (0.0987–0.1024,  $n = 3$  [3]). The mean  $^{187}\text{Os}/^{188}\text{Os}$  values and  $T_{\text{MA}}^{\text{CHUR}}$  ages of the main PGM groups of the Kimberley conglomerate formation (Table 3), obtained using the LA MC-ICP MS method, within the error match the Os-isotopic parameters of PGMs from the Evander goldfield characterized by the N-TIMS method ( $^{187}\text{Os}/^{188}\text{Os} = 0.1053 \pm 0.0001$ ,  $T_{\text{MA}}^{\text{CHUR}} = 3.222$  Ga,  $n = 11$  and  $^{187}\text{Os}/^{188}\text{Os} = 0.1065 \pm 0.0003$ ,  $T_{\text{MA}}^{\text{CHUR}} = 3.060$  Ga,  $n = 8$ , respectively [3, 5]).

Presence of the age-varying PGMs in placers, the formation of which occurred at various tectonomagmatic stages of the geological history of the Earth, is characteristic for many placer deposits [16, 17, 41–46 etc.]. The revealed variability of  $T_{\text{MA}}^{\text{CHUR}}$  ages is consistent with the presence of global stages for PGE mineralization formation controlled by deep geodynamic processes in the mantle [47, 48 etc.]. The coincidence of the Archaean datings for the Witwatersrand goldfields argue for repeated ore-forming processes in the early history of the

Earth. The identified Os-isotopic ages of Ru–Os–Ir–Pt alloys, Ru–Os sulfides and unnamed polycomponent solid solutions of the Ru–Os–Ir–Pt–Fe system from the Kimberley conglomerate formation are the evidence of the clastic (placer) origin of PGE mineralization, confirming the high stability of the Os-isotopic system of PGM to secondary processes, widely manifested within the Witwatersrand Basin.

### Conclusions

The compositional and isotopic characteristics of the studied PGM assemblages are consistent with: (i) high-temperature formation of Ru–Os–Ir–Pt alloys, unnamed polycomponent solid solutions of the Ru–Os–Ir–Pt ( $\pm$  Fe) and Ru–Os sulfides, (ii) similarity of the initial Os-isotope composition in coexisting Os-bearing alloys and Ru–Os sulfides, (iii) subhondritic Archaean source of platinum-group elements and (iv) possibility of using  $^{187}\text{Os}/^{188}\text{Os}$  ages of PGMs to discriminate between models of formation of noble metal mineralization from the Witwatersrand basin. Thus, the identified mineral assemblages containing refractory PGE are a unique source of information on mantle processes in the early history of the Earth.

*Acknowledgments.* This study was supported by RFBR (grant No. 15-05-08332-a) and the Agency of Natural Resources of the Krasnoyarsk Territory (state contract 7F-TAO/2005).

### REFERENCES

- Du Toit A. L. 1954, Geology of South Africa. Edinburgh, London, 611 p.
- Feather C. E. 1976, Mineralogy of platinum-group minerals in the Witwatersrand, South Africa. Economic Geology, vol. 71, pp. 1399–1428.
- Malitch K. N., Merkle R. K. W. 2004, Ru–Os–Ir–Pt and Pt–Fe alloys from the Evander Goldfield (Witwatersrand Basin, South Africa): detrital origin inferred from compositional and osmium isotope data. Canadian Mineralogist, vol. 42, pp. 631–650.
- Merkle R. K. W., Franklyn C. B. 1999, Milli-PIXE determination of trace elements in osmium rich platinum group minerals from the Witwatersrand basin, South Africa. Nuclear Instruments and Methods in Physics Research, vol. 158, pp. 156–161.
- Malitch K. N., Kostyanov A. I., Merkle R. K. V. 2000, *Veschestvennyy sostav i osmievaya izotopiya platinoidnoy mineralizatsii Vostochnogo Vitwatersanda (Yuzhnaya Afrika)* [Material composition and osmium isotopes of PGE mineralization of Eastern Witwatersrand (South Africa)]. *Geologiya rudnykh mestorozhdeniy* [Geology of Ore Deposits], vol. 42, no. 3, pp. 281–295 (in Russian).
- Hart S. R., Kinloch E. D. 1989, Osmium isotope systematics in Witwatersrand and Bushveld ore deposits. Economic Geology, vol. 84, pp. 1651–1655.
- Frimmel H. E., Minter W. E. L. 2002, Recent developments concerning the geological history and genesis of the Witwatersrand gold deposits, South Africa. Society of Economic Geologists. Special Publication 9, pp. 17–45.
- Robb L. J., Davis D. W., Kamo S. L. 1990, U–Pb ages on single detrital zircon grains from the Witwatersrand Basin, South Africa: constraints on the age of sedimentation and on the evolution of granites adjacent to the basin. The Journal of

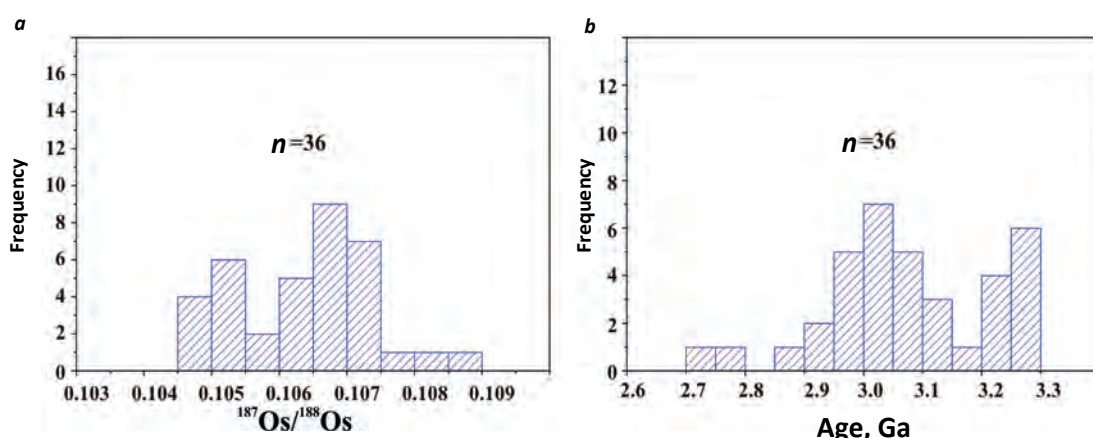


**Figure 4.** Relative probability histograms for: (a) Os-isotopic composition of PGMs and (b) model  $T_{\text{MA}}^{\text{CHUR}}$  age of PGMs from the Kimberley conglomerate formation.

- Geology, vol. 98, pp. 311–328.
9. Robb L. J., Meyer F. M. 1995, The Witwatersrand Basin, South Africa: Geologic framework and mineralization processes. *Ore Geology Reviews*, vol. 10, pp. 67–94.
  10. Tweedie E. B. 1986, The Evander Goldfield. In: *Mineral Deposits of Southern Africa*. Geological Society of South Africa, Johannesburg, vol. 1, pp. 705–730.
  11. Barton E. S., Compston W., Williams I. S., Bristow J. W., Hallbauer D. K., Smith C. B. 1989, Provenance ages for the Witwatersrand Supergroup and the Venterdorp contact reef: constraints from ion microprobe U–Pb ages of detrital zircons. *Economic Geology*, vol. 84, pp. 2012–2019.
  12. Rosman K. J. R., Taylor P. D. P. 1998, Isotopic composition of the elements 1997. *Pure and Applied Chemistry*, vol. 70, pp. 217–235.
  13. Badanina I. Yu., Malitch K. N., Murzin V. V., Khiller V. V., Glavatskikh S. P. 2013, *Mineralogicheskie i geochemicheskie osobennosti platinoidnoy mineralizatsii Verkh-Neyvinskogo dunit-gartsburgitovogo massiva (Srednyi Ural, Rossiya)* [Mineralogical and geochemical features of platinum mineralization of the Verkh-Neyvinsk dunit-harzburgite massif (Middle Urals, Russia)]. *Trudy Instituta geologii i geokhimii imeni akad. A. N. Zavaritskogo UrO RAN* [Proceedings of the Institute of geology and geochemistry named after academician A. N. Zavaritsky], no. 160, pp. 188–192 (in Russian).
  14. Badanina I. Yu., Malitch K. N., Lord R. A., Belousova E. A., Meisel T. C. 2016, Closed-system behaviour of the Re–Os isotope system recorded in primary and secondary PGM assemblages: evidence from a mantle chromitite at Harold's Grave (Shetland ophiolite Complex, Scotland). *Ore Geology Reviews*, vol. 75, pp. 174–185.
  15. Malitch K. N., Melcher F., Muhlhans H. 2001, Palladium and gold mineralization in podiform chromitite at Kraubath, Austria. *Mineralogy and Petrology*, vol. 73, pp. 247–277.
  16. Nowell G. M., Pearson D. G., Parman S. W., Luguet A., Hanski E. 2008, Precise and accurate  $^{186}\text{Os}/^{188}\text{Os}$  and  $^{187}\text{Os}/^{188}\text{Os}$  measurements by Multi-collector Plasma Ionisation Mass Spectrometry, part II: Laser ablation and its application to single-grain Pt–Os and Re–Os geochronology. *Chemical Geology*, vol. 248, pp. 394–426.
  17. Pearson D. G., Parman S. W., Nowell G. M. 2007, A link between large mantle melting events and continent growth seen in osmium isotopes. *Nature*, vol. 449, pp. 202–205.
  18. Harris D. C., Cabri L. J. 1991, Nomenclature of platinum-group-element alloys: review and revision. *Canadian Mineralogist*, vol. 29, pp. 231–237.
  19. Ludwig K. R. 2003, User's Manual for ISOPLOT/Ex 3.00. A Geochronological Toolkit for Microsoft Excel. Berkeley Geochronology Center Special Publication, no. 4, 70 p.
  20. Chen J. H., Papanaastassiou D. A., Wasserburg G. J. 1998, Re–Os systematics in chondrites and the fractionation of the platinum-group elements in the early solar system. *Geochimica et Cosmochimica Acta*, vol. 62, pp. 3379–3392.
  21. Smoliar M. I., Walker R. J., Morgan J. W. 1996, Re–Os ages of group IIA, IIIA, IVA, and IVB meteorites. *Science*, vol. 271, pp. 1099–1102.
  22. Frimmel H. E. 2014, A giant Mesoarchean crustal gold-enrichment episode: Possible causes and consequences for exploration. *Society of Economic Geologists*. Special Publication, vol. 18, pp. 209–234.
  23. Depine M., Frimmel H. E., Emsbo P., Koenig A. E., Kern M. 2013, Trace element distribution in uraninite from Mesoarchean Witwatersrand conglomerates (South Africa) supports placer model and magmatogenic source. *Mineralium Deposita*, vol. 48, pp. 423–435.
  24. Hallbauer D. K., Utter T. 1977, Geochemical and morphological characteristics of gold particles from recent river deposits and the fossil placers of the Witwatersrand. *Mineralium Deposita*, vol. 12, pp. 296–306.
  25. Horscroft F. D. M., Mossman D. J., Reimer T. O., Hennigh Q. 2011, Witwatersrand metallogenesis: The case for (modified) syngenesies. *Society for Sedimentary Geology (SEPM) Special Publication*, vol. 101, pp. 75–95.
  26. Mellor E. T. 1916, The conglomerates of Witwatersrand. *Transactions of the Institution of Mining and Metallurgy*, vol. 25, pp. 226–348.
  27. Minter W. E. L. 1999, Irrefutable detrital origin of Witwatersrand gold and evidence of eolian signatures. *Economic Geology*, vol. 94, pp. 665–670.
  28. Frimmel H. E., Gartz V. H. 1997, Witwatersrand gold particle chemistry matches model of metamorphosed, hydrothermally altered placer deposits. *Mineralium Deposita*, vol. 32, pp. 523–530.
  29. Frimmel H. E., Groves D. I., Kirk J., Ruiz J., Chesley J., Minter W. E. L. 2005, The formation and preservation of the Witwatersrand goldfields, the world's largest gold province. *Economic Geology* 100<sup>th</sup> Anniversary Volume, pp. 769–797.
  30. Barnicoat A. C., Henderson I. H. C., Knipe R. J., Yardley B. W. D., Napier R. W., Fox N. P. C., Kenyon A. K., Muntingh D. J., Strydom D., Winkler K. S., Lawrence S. R., Cornford C. 1997, Hydrothermal gold mineralization in the Witwatersrand basin. *Nature*, vol. 386, pp. 820–824.
  31. Graton L. C. 1930, Hydrothermal origin of the Rand gold deposits. Part I. Testimony of the conglomerates. *Economic Geology*, vol. 25, pp. 1–185.
  32. Phillips G. N., Law J. D. M. 2000, Witwatersrand gold fields: Geology, genesis and exploration. *Society of Economic Geologists Reviews*, vol. 13, pp. 439–500.
  33. Phillips G. N., Powell R. 2011, Origin of Witwatersrand gold: A metamorphic devolatilisation-hydrothermal replacement model. *Transactions of the Institution of Mining and Metallurgy*, Applied Earth Sciences, section B, vol. 120, pp. 112–129.
  34. Kirk J., Ruiz J., Chesley J., Titley S., Walshe J. A. 2001, Detrital model for the origin of gold and sulfides in the Witwatersrand basin based on Re–Os isotopes. *Geochimica et Cosmochimica Acta*, vol. 65, pp. 2149–2159.
  35. Kirk J., Ruiz J., Chesley J., Walshe J., England G. 2002, A major Archean gold and crust-forming event in the Kaapvaal craton, South Africa. *Science*, vol. 297, pp. 1856–1858.
  36. Mathur R., Gauert C., Ruiz J., Linton P. 2013, Evidence for mixing of Re–Os isotopes at <2.7Ga and support of a remobilized placer model in Witwatersrand sulfides and native Au. *Lithos*, vol. 164–167, pp. 65–73.
  37. Schaefer B. F., Pearson D. G., Rogers N. W., Barnicoat A. C. 2010, Re–Os isotope and PGE constraints on the timing and origin of gold mineralization in the Witwatersrand basin. *Chemical Geology*, vol. 276, pp. 88–94.
  38. Cousins C. A. 1973, Platinoids in the Witwatersrand system. *Journal of the South African Institute of Mining and Metallurgy*, vol. 73, pp. 184–199.
  39. Bird J. M., Bassett W. A. 1980, Evidence of a deep mantle history in terrestrial osmium–iridium–ruthenium alloys. *Journal of Geophysical Research*, vol. 85 pp. 5461–5470.
  40. Andrews D. R. A., Brenan J. M. 2002, Phase-equilibrium constraints on the magmatic origin of laurite and Os–Ir alloy. *Canadian Mineralogist*, vol. 40, pp. 1705–1716.
  41. Badanina I. Yu., Malitch K. N., Belousova E. A., Murzin V. V., Lord R. A. 2014, *Osmiye-izotopnaya sistematika Ru–Os–Ir splavov i Ru–Os sul'fidov dunit-gartsburgitovyh massivov: sintez novykh dannyykh* [Osmium-isotopic systematics of Ru–Os–Ir alloys and Ru–Os sulfides from dunit-harzburgite massifs: synthesis of new data]. *Trudy Instituta geologii i geokhimii imeni akad. A. N. Zavaritskogo UrO RAN* [Proceedings of the institute of geology and geochemistry named after academician A. N. Zavaritsky], no. 161, pp. 167–172 (in Russian).
  42. Kostyanov A. I. 1998, *Model'nyi Re–Os vozrast samorodnykh platinovykh mineralov* [Model Re–Os age of native platinum minerals]. *Geologiya rudnykh mestorozhdeniy* [Geology of Ore Deposits], vol. 40, no. 6, pp. 540–545 (in Russian).
  43. Malitch K. N., Badanina I. Yu. 1999, *Khimicheskiy sostav i izotopnye osmirudnye sifery Ru–Os–Ir splavov Kunarskogo dunit-gartsburgitovogo kompleksa (severo-vostochnyy Taymyr, Rossiya)* [Chemical composition and osmium isotopes of Ru–Os–Ir alloys of the Kunar dunit-harzburgite complex (north-eastern Taimyr, Russia)]. *Izvestiya vysshikh uchebnykh zavedeniy. Geologiya i razvedka* [Proceedings of Higher Schools. Geology and Exploration], no. 1, pp. 16–29 (in Russian).
  44. Malitch K. N., Kostyanov A. I. 1999, *Model'nyi Re–Os–Ir vozrast platinoidnoy mineralizatsii Gulinskogo massiva (sever Sibirskej platformy, Rossiya)* [Model Re–Os-age of PGE mineralization of the Guli Massif (north of the Siberian Platform, Russia)]. *Geologiya rudnykh mestorozhdeniy* [Geology of Ore Deposits], no. 2, pp. 143–153 (in Russian).
  45. Okrugin A. V., Kostyanov A. I., Shevchenko S. S., Lazarenkov V. G. 2006, *Model'nyi Re–Os–Ir vozrast mineralov platinovoy gruppy iz "vilyuyskikh" rossyapey vostoka Sibirskej platformy* [Model Re–Os-age of platinum-group minerals from the "Vilyuyskie" placers of the East of the Siberian platform]. *Doklady RAN* [Doklady Earth Sciences], vol. 410, no. 3, pp. 372–375 (in Russian).
  46. Rudashevskiy N. S., Kostyanov A. I., Rudashevskiy V. N. 1999, *Mineralogicheskie i izotopnye svyazi stvora proiskhozhdeniya massivov alpinotipnoy formatsii (na primere Ust'-Bel'skogo massiva, Koryakskoe nador'e)* [Mineralogical and isotope evidences of the origin of the Alpine-type massifs (on the example of the Ust'-Bel'sky Massif, Koryak Upland)]. *Zapiski VMO* [Proceedings of the Russian Mineralogical Society], vol. 128, no. 4, pp. 11–28 (in Russian).
  47. Carlson R. W. 2002, Osmium remembers. *Science*, vol. 296, pp. 475–477.
  48. Drobetsov N. L., Kirdyashkin A. G. 1998, Deep-Level Geodynamics. Swets and Zeitlinger, Rotterdam, Netherlands, 328 p.

**Инна Юрьевна Баданина,**  
innabandanina@yandex.ru  
**Крешимир Ненадович Малич,**  
dunite@yandex.ru  
**Вера Витальевна Хиллер,**  
hilvervit@mail.ru  
Институт геологии и geoхимии УрО РАН  
Россия, Екатеринбург, ул. Академика Вонсовского, 15

**Антон Владимирович Антонов,**  
Anton\_Antonov@vsegei.ru  
**Игорь Николаевич Капитонов,**  
Igor\_Kapitonov@vsegei.ru  
**Светлана Муратовна Туганова**  
Всероссийский научно-исследовательский  
геологический институт  
Россия, Санкт-Петербург, Б. О., Средний просп., 72

**Роланд Карл Вилли Меркль,**  
Университет Претории  
Южная Африка, Претория, Elandsport 357-Jr

**Inna Yur'evna Badanina,**  
innabandanina@yandex.ru  
**Kreshimir Nenadovich Malitch,**  
dunite@yandex.ru  
**Vera Vital'evna Khiller,**  
hilvervit@mail.ru  
Institute of Geology and Geochemistry of the Ural Branch  
of the Russian Academy of Sciences  
Ekaterinburg, Russia

**Anton Vladimirovich Antonov,**  
Anton\_Antonov@vsegei.ru  
**Igor' Nikolaevich Kapitonov,**  
Igor\_Kapitonov@vsegei.ru  
**Svetlana Muratovna Tuganova**  
All-Russian Geological Research Institute  
St. Petersburg, Russia

**Roland Karl Willi Merkle,**  
University of Pretoria  
Pretoria, South Africa